AIAA JOURNAL
Vol. 41, No. 8, August 2003

Reliability-Based Structural Optimization of an Elastic-Plastic Beam

Mazen A. Ba-abbad* and Rakesh K. Kapania†
Virginia Polytechnic Institute and State University, Blacksburg, Virginia 24061-0203
and
Efstratios Nikolaidis‡
University of Toledo, Toledo, Ohio 43606-3390

The application of reliability-based optimization to an elastic-plastic beam is studied. The objective is to demonstrate the benefits of reliability-based optimization over the deterministic optimization in such applications where the design requirements of the member tolerate some plastic behavior. Also, some of the difficulties that one might encounter while performing reliability-based optimization of elastic-plastic beams are addressed. A graphical method was used here to avoid the problems of high nonlinearity and derivative discontinuity of the reliability function. The method starts by obtaining a deterministic optimum design that has the lowest possible weight for a prescribed safety factor, and, based on that design, the method obtains an improved optimum design that has either a higher reliability or a lower weight or cost. In this application three failure modes are considered for an elastic-plastic beam of T cross section under combined axial, bending, and shear loads. The failure modes are based on the beam total plastic failure in a section, buckling, and maximum allowable deflection. The results show that it is possible to get improved optimum designs (more reliable or lighter) using reliability-based optimization as compared to the design given by deterministic optimization. Also, the results show that the reliability function can be highly nonlinear with respect to the design variables with discontinuous derivatives.

Introduction

ALTHOUGH a structural designer has to consider many uncertain factors, such as the variability in the magnitudes of the applied loads and material properties, the field of structural optimization is still dominated by deterministic methods that neglect these uncertainties. Also, in deterministic design safety is measured using a safety factor, which can over- or underestimate the true safety level of a design, thereby producing inefficient or even unsafe designs. Therefore, it is important to incorporate reliability-based concepts in structural optimization.

Saving structural weight and, at the same time, maintaining an acceptable level of safety is critical in many aerospace and naval applications. Therefore, we need to demonstrate that by using reliability-based optimization we might be able to save weight while maintaining an acceptable level of safety.

However, one of the reasons that has slowed the acceptance of the reliability-based optimization by the aerospace industry is that its computational cost is much higher as compared to the cost of employing a deterministic approach to the design of various components. In the case of the deterministic design, the analysis calculations are performed for only one set of parameters to yield the design response to the applied loads and the corresponding safety measure. In reliability-based design, on the other hand, the analysis calculations are repeated several times to calculate the reliability of a design. Hence, there is a need to perform reliability-based optimization by using only a limited number of analyses. A second reason that might have stalled the use of reliability-based optimization is that the reliability-based optimization calculations might not converge all of the time. For instance, Frangopol has pointed out that reliability-based optimization problems were solved with varying degrees of success.[1] (Reference 1 also contains lists of references that cover the development of the reliability-based design during the years 1973–1993.) Moreover, this problem was clearly addressed by Royset et al.,[2] who explained that the reason for this failure is that the reliability function is highly nonlinear and/or not smooth (has discontinuous derivatives), and thus proposed a procedure to avoid this difficulty. Their procedure requires reformulating the reliability-optimization problem in such a way that will make it solvable by semi-infinite optimization methods.[3] Still, Royset et al. concluded that the success of their proposed method depends on how the reliability calculations modify the optimization subproblem.

Wang et al.[4] tried to overcome the reliability function nonlinearity and derivative discontinuity problem by using a piecewise approximation of the reliability function, and they have proposed approximating the design constraints using multivariate splines and then using these splines to perform the reliability-based optimization. However, the spacing between the nodes of the spline needs to be optimized to yield the maximum computational economy. Earlier attempts did not address the issue of nonsmooth objective and constraint functions and used optimization methods that are either based on the derivatives of the reliability function[5–10] or even based on random search of the design space.[11,12]

The objectives of this paper are to 1) perform reliability-based optimization on a representative structural component of a vehicle that is allowed to behave plastically during its service and 2) demonstrate the potential advantages of the reliability-based optimum design over the deterministic optimum design. Also, this application involves multiple failure modes that are nonlinear and thus might result in a highly nonlinear reliability function with possible points of derivative discontinuity, which can cause difficulties during the calculations. We will address these difficulties and present one method to overcome these difficulties. For this purpose we considered the structural optimization of an elastic-plastic beam of T cross section (such as the one used as a plate stiffener in aircraft fuselages or ship decks) under combined axial, bending, and shear loads. The structural optimization of this beam involves setting constraints on

Received 26 July 2002; revision received 17 January 2003; accepted for publication 18 March 2003.

*Graduate Research Associate, Aerospace and Ocean Engineering Department. Student Member AIAA.
†Professor, Aerospace and Ocean Engineering Department. Associate Fellow AIAA.
‡Professor, Mechanical, Industrial and Manufacturing Engineering Department. Member AIAA.

the stresses, the deformations, and the buckling instability that the beam might experience. The stress constraint requires generating load interaction surfaces (or hypersurfaces) for each beam cross section considered by the optimizer. These load interaction surfaces determine the limiting points at which the whole cross section fails plastically. Also, the deformation constraints require determining the deflection of the beam and its buckling behavior each time the cross section is modified by the optimizer.

Researchers have developed different approaches to deal with the limit load analysis of beam sections.[13–19] These approaches vary in the computational efficiency as well as in the range of applicability to loads and cross sections. For instance, Bushnell[14] proposed a strategy for solving problems involving large deflections, elastic-plastic material behavior, and primary creep. However, his work was limited to the bending loads and did not consider the effects of combined loads. The same limitation was found in the works of Yau et al.[15] and Hong.[16] Yu and Hua[17] constructed an interaction surface (also known as yield surface) between the axial, direct shear, and bending loads using the slip-line fields. Still, their approach was limited to beams that approach thin and wide strips, and it is not obvious how their work can be generalized to include torsional loads or even handle practical beams.

Al-Bermani and Kitipornchai[18] have presented a procedure in which they have developed load interaction surfaces for a number of cross sections and used a finite element approach to obtain the corresponding deflections. Gebbeken[19] has presented a numerical approach, which is similar to that of Al-Bermani and Kitipornchai in that it depends on generating the interaction surface and then obtaining the deflection profile using a finite element method. However, the procedures in Refs. 18 and 19 cannot be readily applied to the problem at hand because they require developing an interaction surface for the T section. Also, these methods do not determine the amount by which a constraint is violated for the failed design, and this information is needed for the optimization algorithm to find a feasible design given an initial infeasible design. Thus, there is a need to develop a method to calculate the limit load constraint that is suitable for reliability-based optimization. Moreover, because in the presence of deflection the bending moment might become a function of the applied axial load we need to calculate the bending moment and deflection simultaneously.

The paper begins with the development of mathematical models for determining failure loads corresponding to three failure modes for an elastic-plastic beam of T cross section under combined axial, bending, and shear loads. Next, the deterministic optimization problem is stated, and a deterministic optimization is performed for five safety factors (1.50, 1.75, 2.00, 2.25, and 2.50). After that, the reliability of the deterministic optimum design with SF 1.50 is calculated using both a first-order second-moment method (Hasofer–Lind)[20] and Monte Carlo simulation with importance sampling[21,22] to check for the suitability of applying the first-order second-moment method to this problem. Then, the reliabilities of the other deterministic optimum designs are calculated using the Hasofer–Lind method. Finally, reliability-based optimization is performed to find 1) the most reliable design that has the same weight as that of the deterministic design and 2) the lightest design that has the same reliability as that of the deterministic design. Using the proposed method, we were able to perform reliability-based optimization successfully. The results show that in most cases we were able to obtain improved optimum designs when we used the reliability-based optimization. Also, we address the reasons for not being able to get significant improvements over the deterministic optimum design when such a case occurred.

Limit-Combined Load Analysis and the Interaction Surface

Consider a beam of T cross section under the combination of axial load and bending moment shown in Fig. 1. The objective is to determine the failure loads of this beam. First, the interaction of the axial force and bending moment is considered, and later, the interaction of the shear loads will be included.

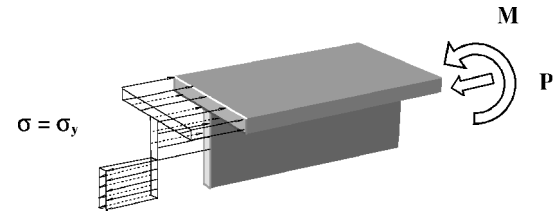

Fig. 1 State of stress for a T beam under the combination of axial load and bending moment that causes the whole cross section to deform plastically.

Failure Under Axial and Bending Stresses

For a linear-elastic material the axial stress can be linearly combined with the flexural stresses until the extreme fibers yield. However, after yielding the failure stresses do not combine linearly, and they can be determined from the equilibrium of forces and moments over the cross section. Let us consider the state of stress at a beam of T cross section under the combination of axial load and bending moment that causes the whole cross section to deform plastically as shown in Fig. 1. From the equilibrium of forces in the axial direction (noting that the axial compressive load P is assumed to be acting at the centroid of the cross section),

$$P = \sigma_y(A_c - A_t) \tag{1}$$

which becomes after simplifying

$$P = \sigma_y(2A_c - A) \tag{2}$$

where P is the applied axial load, σ_y is the yield stress of the material, A_c is the area under compression, A_t is the area under tension, and A is the area of the cross section. Normalizing the axial load by the maximum axial load on the cross section that causes the fully plastic deformation $P_y = \sigma_y A$, the normalized axial load becomes

$$R_p = 2A_c/A - 1 \tag{3}$$

From Eq. (3) solving for A_c, we get

$$A_c = A(R_p + 1)/2 \tag{4}$$

From the force equilibrium and Fig. 1 it can be seen that the axial load at which the flange becomes entirely plastic under compression is an important transition load because the equilibrium equations will change when the net compressive force is distributed entirely on the flange (or portions of it) and when the net compressive force is distributed over the flange and part of the web. We will designate the first situation case a and the second situation case b. Hence, from equilibrium of forces we can get the axial load that causes the flange to become fully plastic under compression. This load after normalization by the maximum axial load and simplification becomes

$$R_{\text{pc}} = \frac{2t_f b}{t_f b + ht_w} - 1 \tag{5}$$

Also, from the equilibrium of the moment we get

$$M = \sigma_y(A_c y_1 + A_t y_2) \tag{6}$$

where y_1 and y_2 are the distances between the centroid of the entire cross section and the centroids of the compression and tension zones, respectively. From the geometry of case a, we can determine the following relations:

$$a_c = \frac{A_c}{b} \tag{7}$$

$$C_c = \frac{a_c}{2} \tag{8}$$

$$C_t = \frac{ht_w(h/2) + (t_f - a_c)b[h + (t_f - a_c)/2]}{ht_w + (t_f - a_c)b} \tag{9}$$

Similarly, for case b

$$a_c = \frac{A_c - t_f b}{t_w} + t_f \tag{10}$$

$$C_c = \frac{t_f b(t_f/2) + (a_c - t_f)t_w(a_c + t_f)/2]}{t_f b + (a_c - t_f)t_w} \tag{11}$$

$$C_t = \frac{h + t_f - a_c}{2} \tag{12}$$

where C_c and C_t are the centroids of the compression and tension zones, respectively, measured from the bottom edge of the web. For both cases the expressions for distances y_1 and y_2 are given by the following relations:

$$y_1 = h + t_f - \bar{Y} - C_c \tag{13}$$

$$y_2 = \bar{Y} - C_t \tag{14}$$

where $\bar{Y}$ gives the location of the centroid of the entire cross section measured from the bottom edge of the web.

We can normalize the moment by the maximum elastic moment M_e that the cross section can experience before any plastic deformation in the extreme fiber sets in. This moment is given as

$$M_e = \sigma_y I/\bar{Y} \tag{15}$$

Then the normalized moment becomes

$$R_m = (A_c\bar{Y}/I)y_1 + [(A - A_c)\bar{Y}/I]y_2 \tag{16}$$

We can now substitute the value of A_c from Eq. (4) into Eq. (16) and obtain two expressions that relate R_p with R_m and the cross-section dimensions for cases a and b. These two expressions will be of the form

$$R_m = f_a(R_p) \tag{17a}$$

$$R_m = f_b(R_p) \tag{17b}$$

The first expression is valid for axial loads in the range from zero to R_{pc} [Eq. (5)]; the second expression is valid for loads higher than R_{pc}. The obtained expressions were applied to the example presented by Smith and Sidebottom[23] and gave identical results. Thus, we have obtained the interaction curve between the axial force and bending moment, and now we will consider the effects of the shear loads.

Effect of Transverse Shear Stress

Transverse shear stresses caused by a bending load have relatively small contribution to the failure of the cross section compared to the bending or torsional shear stresses for long and slender beams (having height to length ratio > 0.3). However, we can include their contribution to failure in case we found that they reduced significantly the yield strength of the material. In that case the new failure stress becomes

$$\sigma_f = \sqrt{\sigma_y^2 - 3\tau^2} \tag{18}$$

where σ_f is the failure stress of the material, σ_y is its yield strength, and τ the average shear stress on the beam cross section.

However, it is important to note the limitation on this reduction factor as it is only valid for shear stresses up to 30% of the axial stresses caused by flexure loads.[24]

Effects of Torsional Shear Stresses

Finally, we include the effect of the torsional shear stress on the total plastic failure of the beam and construct the interaction surface. These torsional effects include the thickness shear stresses (St. Venant's shear stress) and the warping axial stresses (contour stresses). However, the warping axial stresses have secondary effect in a thin walled section and can be ignored.[25]

Now, we need to determine the value of the maximum torque that will deform the entire cross section plastically. We will apply the Nadai sand heap analogy to the cross section and obtain the following expression for the maximum shear stress that the cross section can withstand with no other stresses present[26]:

$$T_p = \tau_y\left(-t_f^3/6 - t_w^3/12 + t_f^2 b/2 + t_w^2 h/2 + t_w^2 t_f/6\right) \tag{19}$$

where (from the Von Mises yield criterion)

$$\tau_y = \sigma_y/\sqrt{3} \tag{20}$$

We can normalize the plastic torque by the maximum elastic torque, that is, the torque after which the extreme fiber deforms plastically:

$$T_e = \frac{\tau_y J}{t_w} = \frac{\tau_y\left(ht_w^3 + bt_f^3\right)}{3t_w} \tag{21}$$

Finally, we obtain the normalized maximum plastic torque for this cross section:

$$R_{T_0} = \frac{T_p}{T_e} = \frac{t_w\left(2t_f^2 + t_w^3 - 6t_f^2 b - 6t_w^2 h - 2t_w^2 t_f\right)}{-4\left(ht_w^3 + bt_f^3\right)} \tag{22}$$

So far, we have developed an interaction curve between the axial force and bending moment, and we have derived an expression for the maximum torsional shear stress for the cross section. We still need to relate all of these quantities together in one constraint. However, we do not need a rigorous mathematical formulation to relate these loads to the limit combined load, but instead we can use a suitable empirical formulation. This empirical formulation must satisfy the convexity condition (Drucker's postulate) and must not assume that the material will bear stresses that are higher than the allowable Von Mises stresses at any point in the cross section.[19,27,28] With this in mind, let us assume that the interaction of the torsional load with both the axial load and the bending moment can be represented by a ruled surface as shown in Fig. 2a. This surface is constructed by extending straight lines from the maximum normalized torsional load to the normalized interaction curve between the bending and the axial load. This way the convexity of the failure surface is assured (because we are using straight lines). Also, no concavity is allowed to occur at any portion of the surface (otherwise the plastic work will be negative), which means that we are at the lower bound of any possible interaction curve between the torsional shear and the other loads. Therefore, at no point in the cross section does the stress exceed the yield strength of the material, which fulfills the second condition that the yield surface must satisfy.

Now, we need to obtain the factor of safety against failure determined by this surface, which tells us how far or near we are from the constraint corresponding to failure of a beam section. Let us assume the projection of any point inside (or outside) the failure surface onto the M–P plane to be denoted by P_1, and let us draw a vector $\boldsymbol{V}_1$ from the origin to the projected point (see Fig. 2b). Then let us extend the vector $\boldsymbol{V}_1$ until it intersects the M–P interaction curve and name the new vector $\boldsymbol{V}_2$. Now, let R_{PM} be the ratio of the lengths:

$$R_{\mathrm{PM}} = \|\boldsymbol{V}_1\|/\|\boldsymbol{V}_2\| \tag{23}$$

which will allow us to obtain the safety factor γ after solving for it from the failure surface equation (24):

$$\gamma R_{\mathrm{PM}} + \gamma R_T = 1 \tag{24}$$

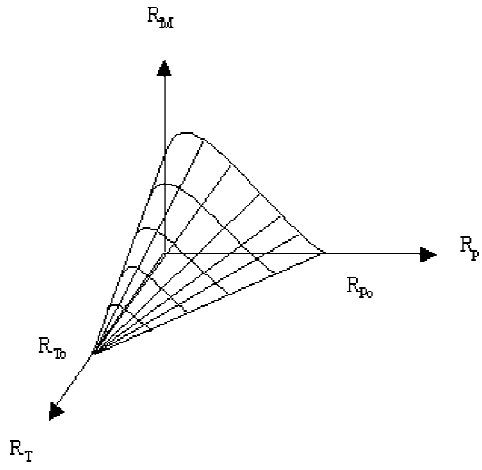

Fig. 2a Safe design zone (under the yield surface) that combines the axial, bending, and torsional shear loads.

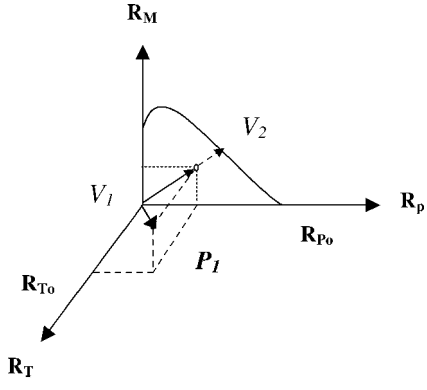

Fig. 2b Projection of the design point on the *M–P* plane.

Beam Plastic Deflection Under the Combined Loads

Here, we are not considering the deflection of the beam under any combination of loads that falls at the interaction surface or beyond because failure by buckling is expected to occur before that. Instead, we are setting a limit for the maximum deflection of the beam (in our case 10% of the total depth of the beam). Moreover, we will assume that the applied loads on the beam do not change with the magnitude of the deflection. Consequently, we do not expect any change in the load distribution over the beam. Also, the high shear modulus of elasticity of structural materials minimizes the effect of the rotation about the Z axis of the beam (caused by torsion) on the reduction of the effective moment of inertia. Therefore, we will only consider the effect of the flexure and buckling loads on the beam deflection.

Although we could have used a general-purpose finite element code to calculate the deflection, it was more economical to write a nonlinear beam finite element code for this problem. Thus, we have used the beam element developed by Yang and Saigal[29] and yang[30] with some modifications to the method in which the unbalanced loads are calculated, to the step size used, and to the convergence criterion. We calculated the axial load and the bending moment directly from the strain distribution over the cross section instead of the iterative procedure that was used in Refs. 29 and 30. Also, we used a fixed incremental displacement that was 1% of the maximum elastic displacement of the beam and stopped the iterations at 95% loss of the beam stiffness to speed up calculations. The results of the present code were in excellent agreement with those of Yang and Saigal.[29]

Out-of-Plane Buckling

The out-of-plane buckling (buckling in the plane of the flange) was considered to prevent the optimizer from obtaining narrow beams that can buckle out of plane. We used Euler's beam buckling formula for this purpose.

Deterministic Structural Optimization

To understand the advantages and disadvantages of the reliability-based optimization, we will compare it with a number of deterministic optimum designs with different safety factors. The intent here is to compare the deterministic optimum designs' weight and safety level to those of reliability-based optimum designs.

Deterministic optimization problem formulation:

$$\begin{gathered}\text{Find}, \boldsymbol{X} \\ \min W(\boldsymbol{X}) \\ s.t. \\ G_i(\boldsymbol{X}) \geq 0 \\ \boldsymbol{X} \geq \boldsymbol{X}^L\end{gathered}$$

where $W(\boldsymbol{X})$ is the weight of the beam, $\boldsymbol{X}$ is the vector of design variables (height of the web, the width of the flange, and their thicknesses as shown in Fig. 3), $G_i(\boldsymbol{X})$ are the constraints, and $\boldsymbol{X}^L$ are the lower limits of the design variables. The constraints are as follows:

1) The first is strength constraint that prevents failure by total plastic deformation at any cross section of the beam: the beam can sustain the applied loads without total plastic deformation at any cross section [$\gamma \geq 1.0$ in Eq. (24)], which is specified by the performance function $G_1(\boldsymbol{X})$.

2) The second is constraint about out-of-plane stability that prevents failure by loss of out-of-plane stability: the beam would not buckle out of plane, which specifies the performance function $G_2(\boldsymbol{X})$.

3) The last is design constraint that prevents failure by excessive in-plane deflection: the in-plane deflection of the beam will not exceed 10% of its total depth, which specifies the performance function $G_3(\boldsymbol{X})$.

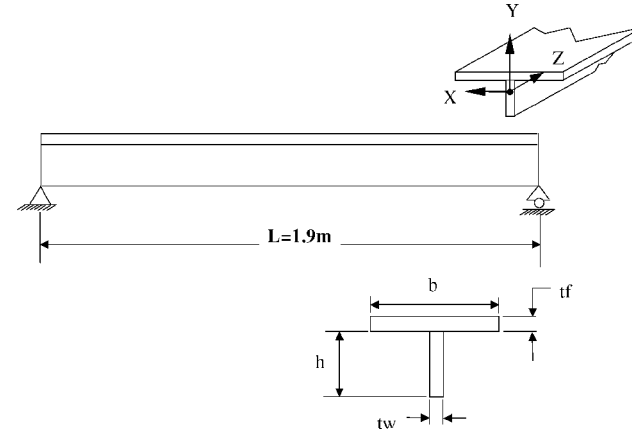

Fig. 3a Geometry and dimensions of the T beam.

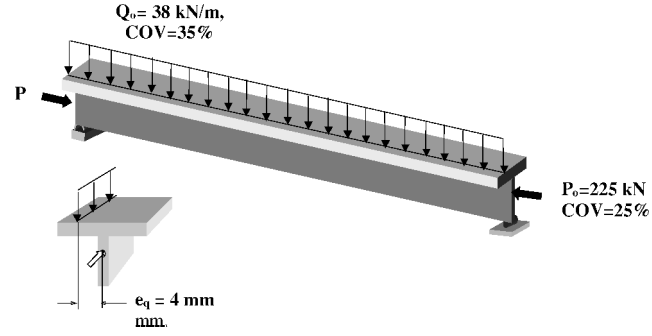

Fig. 3b Loads applied to the beam.

Also, the lower limits on the design variables are manufacturing constraints that prevent the thickness from being less than 5 mm for any portion of the beam.

For the optimization process we have used the Modified Method of Feasible Directions and the sequential quadratic programming optimization algorithms[31] of Visual Doc software.[32] Both methods converged to the same optimum design in the examples considered.

Reliability-Based Structural Optimization

Two formulations of the reliability-based optimization problem will be considered, design for maximum reliability and design for minimum weight. Design for maximum reliability is used if the objective is to find the design with highest reliability (probability of survival) whose weight does not exceed a maximum acceptable limit. In this formulation objective function is the beam reliability. On the other hand, design for minimum weight is used when the objective is to find the lightest beam design whose reliability is no less than a minimum acceptable value. In this formulation objective function will be the beam weight. We will use both approaches and compare the obtained designs to the deterministic optimum design. The beam reliability is a function of the failure modes considered earlier, which are the constraints in the deterministic optimization problem. Manufacturing constraints are considered as side constraints and will not affect the calculation of the design reliability.

Formulations of Reliability-Based Optimization Problems

1) Design for maximum reliability:

$$\begin{gathered} \text{find } \boldsymbol{X} \\ \max R(\boldsymbol{X}) \\ s.t. \\ W(\boldsymbol{X}) \le W_d^* \\ \boldsymbol{X} \ge \boldsymbol{X}^L \end{gathered}$$

where $R(X)$ is the system reliability of the beam, which is the probability of survival of the beam under the applied loads [calculated against the already determined failure modes $G_i(\boldsymbol{X})$], $W(\boldsymbol{X})$ is the weight of the beam, and W_d^* is the weight of the corresponding deterministic optimum design.

2) Design for minimum weight:

$$\begin{gathered} \min W(\boldsymbol{X}) \\ s.t. \\ R(\boldsymbol{X}) \ge R_d^* \\ \bar{\boldsymbol{X}} \ge \boldsymbol{X}^L \end{gathered}$$

where R_d^* is the reliability of the corresponding deterministic optimum design.

Methods Used to Calculate the Reliability of the Beam

To carry out the reliability-based optimization, we need to calculate the reliability of different beam designs under variable loads and/or material properties. Thus, for this application it would be suitable to use a very economical method to calculate the reliability of a design, such as the first-order second-moment methods,[33] and in the case of normally distributed variables we can directly use the Hasofer–Lind (H-L) method (otherwise we might need to transform the random variables into equivalent normal variables).[20] The H-L method requires transforming the random variables and limit-state functions into a new space (space of reduced variables) with independent, normal random variables with zero mean and unit standard deviation. Then, we need to find the most probable failure point, which is the closest failure point to the origin in the space of reduced variables.[31] Finding the most probable failure point for nonlinear state functions is an optimization problem. Thus, it would be worthwhile to check the accuracy of the results by comparing them to those by another more direct method. We chose Monte Carlo simulation with importance sampling because using the direct Monte Carlo simulation needs around 10^7 sample points to for a reliability of 0.999 and a radius of confidence of 1% (Ref. 20). Also, to simplify the reliability calculations we will calculate the probability of failure for each failure mode separately and then use the summation of the probabilities of failure for all of the failure modes as an upper bound on the system probability of failure.[21] Once the beam reliability at different design points is calculated, we can use a suitable optimization scheme to find the reliability-based optimum design.

Reliability-Based Optimization Method

As was mentioned earlier, we needed to devise an efficient method that will enable us to determine the optimum designs for the two reliability-based optimization problems. Although the weight of the beam is a simple function of the design variables, the reliability of the beam is an implicit function of the design variables and might not always be differentiable. Hence, one might not expect that we can use one of the standard optimization algorithms to obtain the reliability-based optimum designs. In light of this, one might think of other optimization tools that will be both economical and can easily overcome the discontinuity in the derivatives of the constraint and/or the objective functions. Thus, we have turned to the sensitivity analysis of the beam in the sense that the effect of each design variable on both the objective function and the constraint is studied separately. This analysis was used to identify two groups of important variables: those that significantly affect the weight and those that affect significantly the reliability. This allows us to perturb the design from the deterministic optimum to either increase the reliability of the design with the least increase in the cost or to reduce the cost with the minimal reduction in reliability. To achieve this, we can vary one design variable at a time and study its effect on both the reliability and the weight of the beam. To save the unnecessary effort, this analysis can be performed in the neighborhood of the optimum deterministic design with the goal of improving its reliability or reduce its cost. Using this information, the optimization problem is then changed into a simple one-dimensional search problem that can be solved graphically.

Numerical Application

We chose a beam of T cross section, which is commonly used as a stiffener in aerospace, ship, and automotive industries. The geometry and dimensions of the beam are shown in Fig. 3a. The loads applied to the beam are an axial compressive load applied to the beam's centroid and a uniform lateral distributed load with an eccentricity of 4 mm, as shown in Fig. 3b. Both the axial load P and the distributed lateral load Q_0 are random, having normal probability distribution with mean values 225 kN and 38 kN/m, respectively, and coefficients of variation given as 25 and 35%, respectively. The material is assumed to behave as elastic-plastic with yield strength of 400 MPa and modulus of elasticity of 70 GPa.

Combined Load and Deflection Analysis

The following should be considered in failure analysis of the beam in this example:

1) The applied bending moment M_{ext} will be a function of the applied loads, and the resulting deflection will have the following form:

$$M_{\text{ext}} = P\delta - Q_0(z^2/2) + (Q_0 L/2)z \tag{25}$$

where δ is the beam deflection in the y direction and L is the length of the beam.

2) If any portion of the beam cross section yields, then the beam bending stiffness is reduced, and thus the beam can fail and lose its capacity to bear more load even before reaching the yield surface (see Figs. 4a and 4b). This situation might not occur for other boundary conditions, such as fixed-end beams, because in that case the beam can continue carrying the load until the yield surface has been reached. Thus, we have modified our constraint formulation accordingly and replaced the limit combined load constraint with the maximum load fraction that the beam can experience before going into bifurcation buckling. However, to avoid getting singularities in the stiffness matrices we limited iterations up to 95% of stiffness reduction of the beam. That is the load at which the slope of the load-deflection curve is less than 5% of its initial value (i.e.,

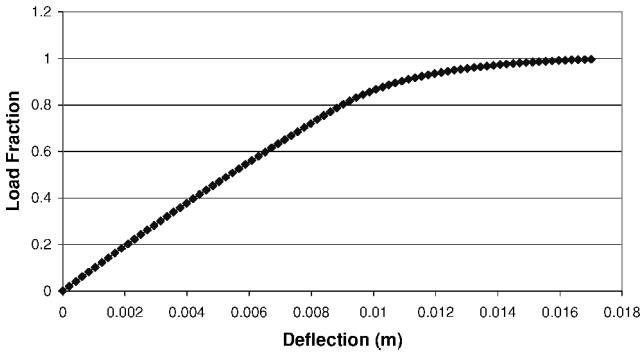

Fig. 4a Load-deflection curve for a T beam, used here under axial and lateral loads.

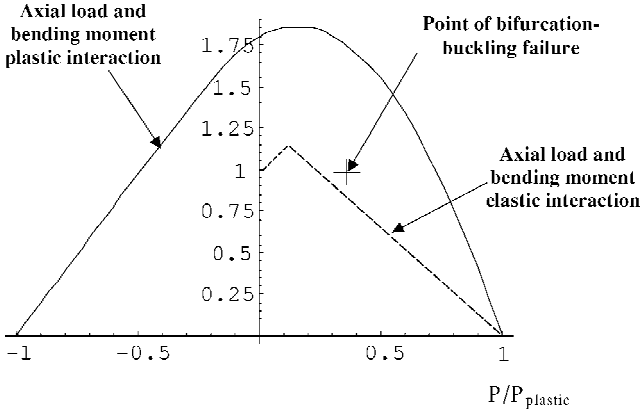

Fig. 4b Location of the failure point on the axial load-bending moment interaction curve.

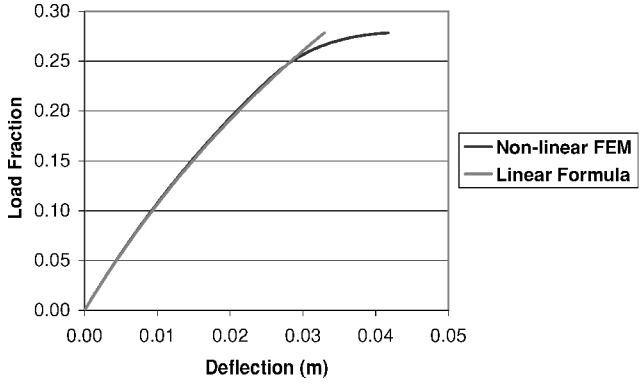

Fig. 5 Comparison between the results of nonlinear finite element method (FEM)[28] and the linear elastic formula [Eq. (26)].

when the beam loses 95% of its stiffness). Also, this observed loss of stiffness occurs much earlier than that predicted by the linear elastic beam-column equation given next,[34] and the maximum deflection obtained at the midspan ($\delta_{\max}$) is greater (Fig. 5).

$$\delta_{\max} = \frac{Q_0}{EIk^4}\left[\sec\left(\frac{kL}{2}\right) - 1\right] - \frac{Q_0 L^2}{8EIk^2}, \qquad k = \sqrt{\frac{P}{EI}} \tag{26}$$

where I is the cross-section moment of inertia and E is the material modulus of elasticity. These results emphasize the importance of considering the inelastic behavior of the beam.

3) The shear loads vary linearly along the beam and vanish at the midspan.

Deterministic Optimum Designs

We have first performed deterministic optimization for safety factors (SF) of 1.50, 1.75, 2.00, 2.25, and 2.50. The results are shown in Table 1. Also, to check whether the obtained designs from optimization were global optima we perturbed the values of the design variables of the designs, and we arrived at the same optimum design every time.

Table 1 Deterministic optimum designs for various safety factors

Factor of safety	Mass, kg	h, mm	t_w, mm	b, mm	t_f, mm
1.50	10.82	244	5	162	5
1.75	11.69	269	5	170	5
2.00	12.53	292	5	178	5
2.25	13.34	317	5	185	5
2.50	14.17	341	5	191	5

Table 2 Probabilities of failure for the deterministic optimum designs (SF of 1.5, 1.75, 2.00, 2.25, and 2.50)

Factor of safety	Failure modes			System
	G_1	G_2	G_3	
1.50	$1.10E-2$	$2.09E-2$	$4.02E-3$	$3.6E-2$
1.75	$2.03E-4$	$1.47E-3$	$8.73E-7$	$1.67E-3$
2.00	$1.07E-6$	$3.01E-5$	$1.09E-13$	$3.12E-5$
2.25	$7.4E-10$	$3.07E-7$	$3.0E-25$	$3.08E-7$
2.50	$1.5E-13$	$1.94E-9$	$3.3E-44$	$1.94E-9$

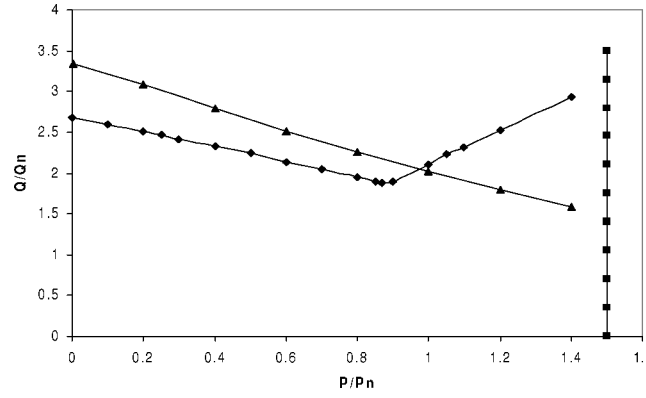

Fig. 6 Boundary performance functions $G_1(X) = 0$, $G_2(X) = 0$, and $G_3(X) = 0$, plotted on the random loads plane. The loads are normalized by their mean values: ♦, $G3$; ■, $G2$; and ▲, $G1$.

Now, before calculating the respective probabilities of failure of these deterministic optimum designs we might need to check on the suitability of the H-L method used to calculate the probabilities of failure in our application. For this purpose we chose the design with the lowest safety level (highest probability of failure), which is the deterministic optimum design for SF = 1.50. We have obtained the probabilities of failure for the three performance functions using Monte Carlo simulation with importance sampling and by using the H-L method. They were in reasonable agreement. The probability of failure for function G_1 using Monte Carlo simulation with importance sampling (IS) is $1.0E-2$ and using H-L it is $1.10E-2$; for function G_2 using IS it is $2.1E-2$ and using H-L it is $2.09E-2$; and for function G_3 using IS it is $1.3E-3$ and using H-L it is $4.02E-3$. Also, we have plotted the three limit state functions $[G_i(X) = 0]$ on the load space to see their degree of nonlinearity and to check for the existence of local minima (Fig. 6). These limit state functions did not show a high level of nonlinearity, nor did they have a local minimum. These trends show that it would be adequate to use the H-L method to calculate the reliability of the T beam. However, the deflection limit state function $[G_3(X) = 0]$ was not monotonic, which is because certain load ratios (axial/lateral) produce more deflection before the buckling failure than the others. Finally, we obtained the probabilities of failure for the other deterministic optimum designs (SF of 1.75, 2.00, 2.25, and 2.50) for the three failure modes, and they are listed (along with the results of SF 1.50) in Table 2.

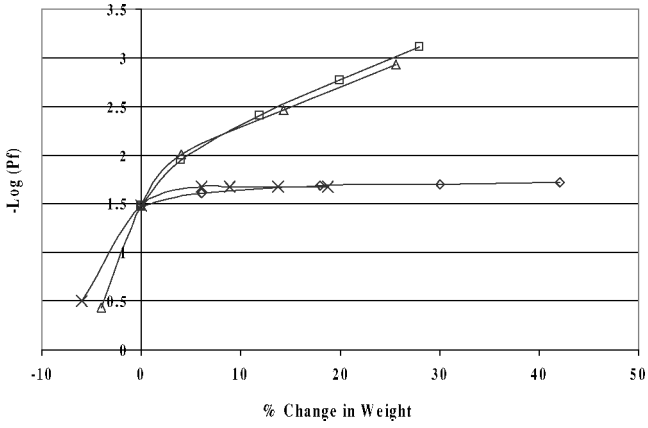

Fig. 7a Effects of varying the design variables on the weight and probability of failure of the deterministic optimum (SF-1.50): ◇, *tw*; □, *tf*; △, *b*; and ×, *h*.

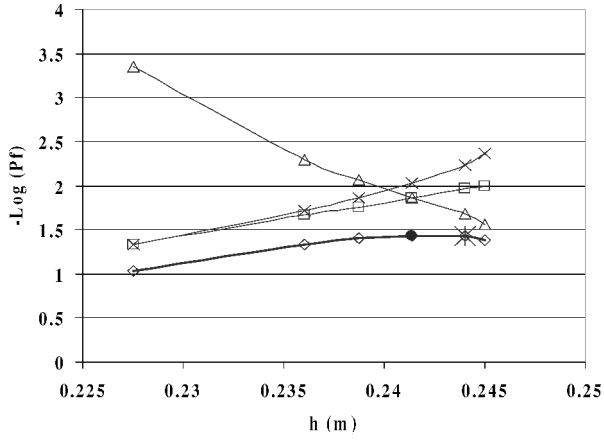

Fig. 7b Searching for the optimum design that has the lowest probability of failure P_f: ◇, system; □, *G*1; △, *G*2; ×, *G*3; ✱, Det SF 1.5; and ●, rel-based optimum.

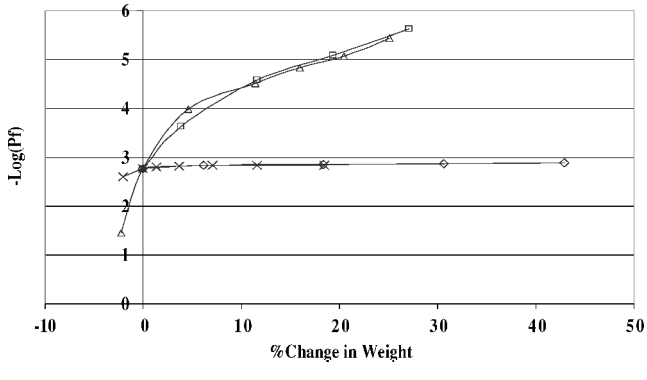

Fig. 8a Effects of varying the design variables on the weight and probability of failure of the deterministic optimum (SF-1.75): ◇, *tw*; □, *tf*; △, *b*; and ×, *h*.

Reliability-Based Optimum Designs

We have performed a sensitivity analysis around each deterministic optimum design. Specifically, we have varied each design variable around the deterministic optimum and plotted the beam probability of failure against the percent increase in weight. This allowed us to determine which design variables we should increase to get the maximum increase in reliability (Figs. 7a–11a). We used this information to solve both reliability-based structural optimization problems, design for maximum reliability and design for minimum weight. Initially, we planned to vary each design variable around ±10% of its value, but we later modified this range during calculations according to the contribution of each design variable to the reliability and weight of the design. Also, because the thicknesses of the flange and the web were constrained to be no less than 5 mm we studied the sensitivity for values above that limit up to 15%. In addition, we used quadratic interpolation between the points. Following are the results of reliability-based optimization starting from the corresponding deterministic design for safety factors of 1.50, 1.75, 2.00, and 2.25.

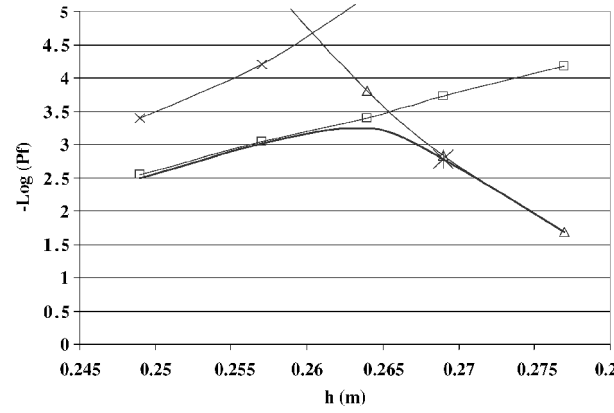

Fig. 8b Searching for the optimum design that has the lowest probability of failure P_f: ——, system Pf; □, *G*1; △, *G*2; ×, *G*3; and ✱, Det SF 1.75.

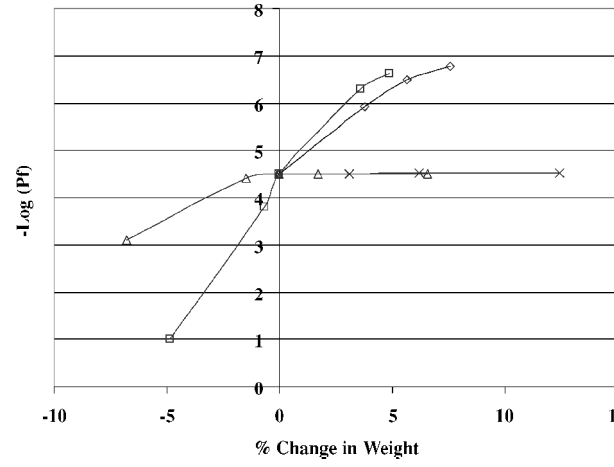

Fig. 9a Effects of varying the design variables on the weight and probability of failure of the deterministic optimum (SF-2.00): ◇, *tf*; □, *b*; △, *h*; and ×, *tw*.

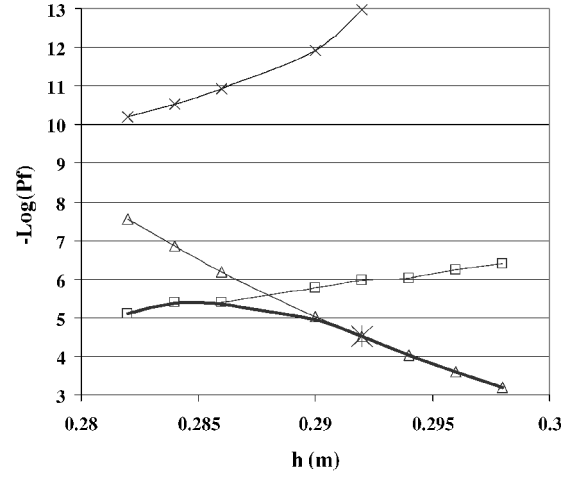

Fig. 9b Searching for the optimum design that has the lowest probability of failure P_f: ——, system; □, *G*1; △, *G*2; ×, *G*3; and ✱, Det SF 2.00.

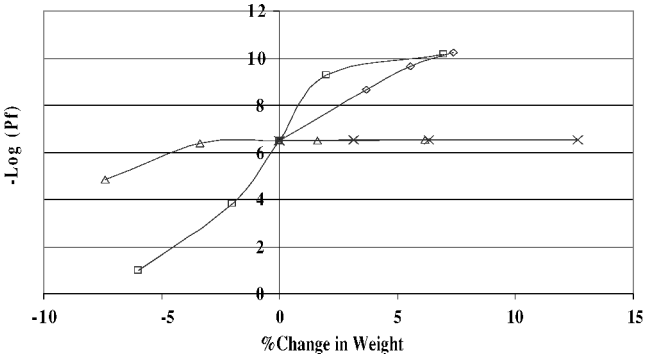

Fig. 10a Effects of varying the design variables on the weight and probability of failure of the deterministic optimum (SF-2.25): ◇, *tf*; □, *b*; △, *h*; and ×, *tw*.

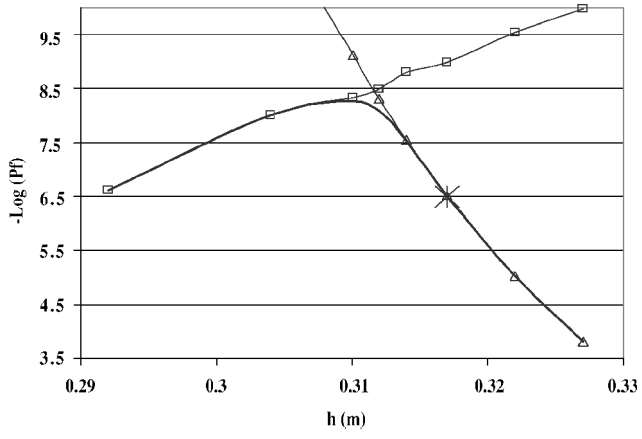

Fig. 10b Searching for the optimum design that has the lowest probability of failure P_f: ——, system; □, *G*1; △, *G*2; ×, *G*3; and ✱, Det SF 2.25.

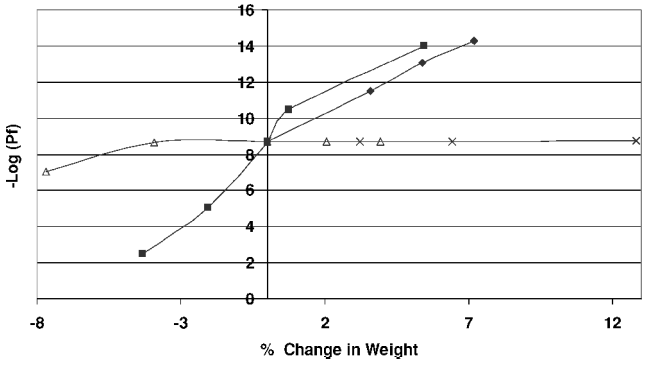

Fig. 11a Effects of varying the design variables on the weight and probability of failure of the deterministic optimum (SF-2.50): ♦, *tf*; ■, *b*; △, *h*; and ×, *tw*.

Deterministic Optimum Design with SF 1.50

Figure 7a shows the reliability of the deterministic optimum design as a function of the weight when the each of the four dimensions of the cross section is changed—one at a time—while the other three dimensions are fixed at their respective values corresponding to the deterministic optimum design. The flange width b is the most important design variable for −4 to 10% change in the design weight, whereas the web thickness t_w has the least effect within that range (Fig. 7a). However, because the web thickness was at its lower limit we chose the web height h to be the variable to be reduced. Now, for the design for maximum reliability we can improve the reliability of the design for the same weight by increasing the flange width and reducing the web height in a way that the weight remains the same. However, the improvement was insignificant, but at least

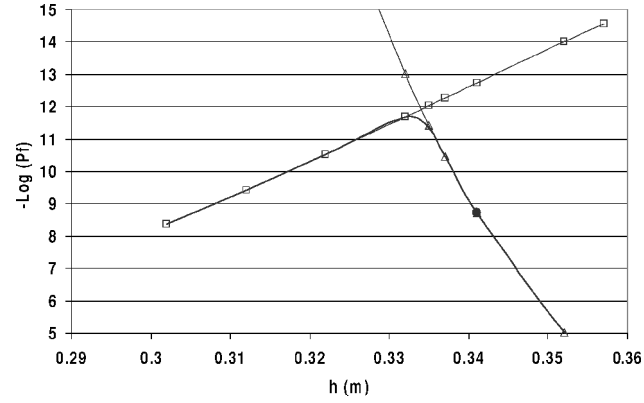

Fig. 11b Searching for the optimum design that has the lowest probability of failure P_f: ——, system; □, *G*1; △, *G*2; ×, *G*3; and ●, Det SF 2.50.

it achieved a more equal balance between different failure modes (Fig. 7b). Consequently, for the second optimization problem it was unlikely to obtain a design with a weight less than the weight of the deterministic optimum design.

Deterministic Optimum Design with SF 1.75

The flange width b is the most important design variable for −4 to 10% change in the design weight, whereas the web height h has the least effect within that range (Fig. 8a). For the first reliability-optimization problem we have improved the reliability of the design for the same weight by increasing the flange width and reducing the web height (Fig. 8b). The situation was favorable for the second optimization problem, and we were able to save about 1.5% of the weight without reducing reliability.

Deterministic Optimum Designs with SF 2.00, 2.25, and 2.50

These three designs showed similar trends as in the deterministic design with SF 1.75 (Figs. 9a–11a), and we were able to improve their respective values of the reliability from $(1.0–3.0 \times 10^{-7})$ to $(1.0–5.0 \times 10^{-9})$, from $(1.0–3.1 \times 10^{-5})$ to $(1.0–4.1 \times 10^{-6})$, and from $(1.0–2.0 \times 10^{-9})$ to $(1.0–2.0 \times 10^{-12})$, respectively. Also, we were able to save weight by 1.27, 3.6, and 5.2%, respectively. Figures 12a and 12b summarize these findings.

Discussion of Reliability-Based Optimization Results

From Table 2 we observe that the reliability of the beam designed deterministically for a factor of safety of 1.50 is rather low (<0.97). This shows that the factor of safety might not be an adequate method to describe the level of safety of a design. Figures 7a–11a provide an insight into the behavior of the reliability and the weight of the beam as functions of each design variable. In addition, looking at Figs. 7–11, one might notice the discontinuity of the beam reliability function and how the contribution of each design variable to the reliability of the beam might differ before and after this discontinuity. Moreover, looking at Figs. 7b–11b we can see that the location of the deterministic optimum designs in the space of the reliability-design variables is located near just one failure mode. This is because the deterministic optimizer stops as soon as it reaches any of the constraints and no further improvement in the objective function is possible. Thus, the risk of failure might not be evenly distributed among the failure modes, and further improvement of the design (by making it more reliable or obtain one with less weight) might be possible by redistributing the material to more equal risks of failure among the three failure modes.

Finally, as we can see from Figs. 12a and 12b, the benefits of the reliability-based optimization over the deterministic optimization increase for higher safety levels, and the increase in benefits is monotonic as found in an earlier study on the design of aircraft wings subject to gust loads.[35] This is because as the safety level of the design increases more material can be used, and thus a better distribution of the material can yield higher benefits.

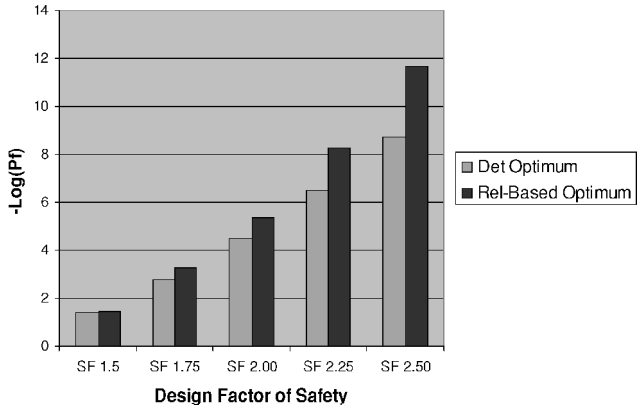

Fig. 12a Comparing the reliability of the deterministic and the reliability-based optimum designs.

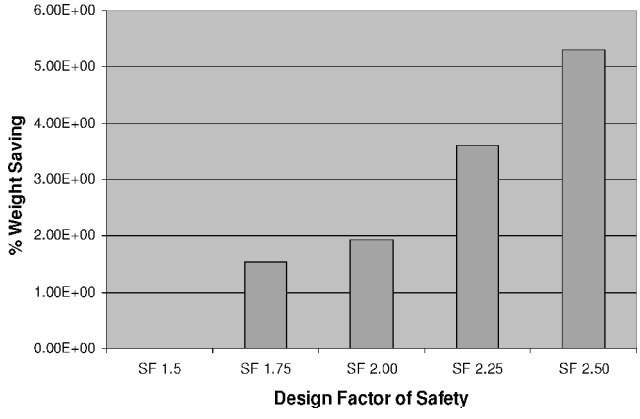

Fig. 12b Weight saving with reliability-based design over the deterministic design.

Conclusions

An elastic-plastic beam design of T cross section under combined loads was optimized. Three failure modes were considered: failure caused by yielding of the entire beam cross section under the combined action of axial and lateral loads, buckling in the plane of the flange, and excessive deflection in the plane of the web. A load interaction surface was constructed to determine the limit load that combines axial, bending, and shear loads. Also, a nonlinear finite element procedure was used to determine the deflection of the beam in the plastic range. Next, deterministic optimization was carried out to find the lightest beam design that can support the applied loads for a given safety factor. The deterministic optimization was repeated to obtain optimum designs for a number of different safety factors. Then, the probability of failure was calculated for each deterministic optimum design using 1) Monte Carlo simulation with importance sampling and 2) first-order second-moment methods. Finally, reliability-based optimization was performed to find 1) the lightest design that has same reliability as the deterministic design and 2) the most reliable design that has same weight as the deterministic design.

The results show that the reliability-based optimization can obtain designs with lower probability of failure than the designs obtained by the deterministic optimization. Consequently, this advantage can be used to obtain safer designs that have the same weight as the deterministic optimum designs or designs that have less weight and the same probability of failure as the deterministic ones. Also, these results show we were able to deal with the problem of high nonlinearity and derivative discontinuity of the reliability function in such a way that allowed us to obtain an improved design over the deterministic design in most cases.

Acknowledgments

The authors thank all of those who supported this work and helped in its success, especially the U.S. Marine Corps, who supported portions of this work under Phase II STTR Contract M67854-00-C-3050 awarded to ADOPTECH with Virginia Polytechnic Institute and State University as a subcontractor, and Scott Ragon of ADOPTECH, Inc., who provided a significant number of technical comments toward the eventual success of this work. Also, the authors express thanks to Tom Stoumbos of General Dynamics Amphibious Marine Systems of Woodbridge, Virginia, for his technical support; Zafer Gurdal and Eric Johnson of Virginia Polytechnic Institute and State University's Department of Aerospace and Ocean Engineering for their critique; and John Coggin for his comments.

References

[1]Frangopol, D. M., "Reliability-Based Optimum Structural Design" *Probabilistic Structural Mechanics Handbook: Theory and Industrial Applications*, edited by C. Raj Sundararajan, Chapman and Hall, New York, 1995, pp. 352–387.

[2]Royset, J. O., Der Kiureghian, A., and Polak, E., "Reliability-Based Optimal Design of Series Structural Systems," *Journal of Engineering Mechanics*, Vol. 127, No. 6, 2001, pp. 607–614.

[3]Polak, E., *Optimization: Algorithms and Consistent Approximations*, Springer-Verlag, New York, 1997, p. 368.

[4]Wang, L., Grandhi, R. V., and Hopkins, D. A., "Structural Reliability Optimization Using an Efficient Safety Index Calculation Procedure," *International Journal for Numerical Methods in Engineering*, Vol. 38, 1995, pp. 1721–1738.

[5]Nikolaidis, E., and Burdisso, R., "Reliability Based Optimization: a Safety Index Approach," *Computers and Structures*, Vol. 28, No. 6, 1988, pp. 781–788.

[6]Pu, Y., Das, P. K., and Faulkner, D., "A Strategy for Reliability-Based Optimization," *Engineering Structures*, Vol. 19, No. 3, 1997, pp. 276–282.

[7]Nakib, R., "Deterministic and Reliability-Based Optimization of Truss Bridges: A Technical Note," *Computers and Structures*, Vol. 65, No. 5, 1997, pp. 767–775.

[8]Nikolaidis, E., and Stroud, W. J., "Reliability-Based Optimization: A Proposed Analytical-Experimental Study," *AIAA Journal*, Vol. 34, No. 10, 1996, pp. 2154–2161.

[9]Rajagopalan, H. S., and Grandhi, R. V., "Reliability Based Structural Optimization in X Windows Environment," *Computers and Structures*, Vol. 60, No. 1, 1996, pp. 1–10.

[10]Li, W., and Yang, Li, "An Effective Optimization Procedure Based on Structural Reliability," *Computers and Structures*, Vol. 52, No. 5, 1994, pp. 1061–1067.

[11]Cheng, G., Li, G., and Cai, Y., "Reliability-Based Structural Optimization Under Hazard Loads," *Structural Optimization*, Vol. 16, 1998, pp. 128–135.

[12]Natarajan, K., and Santhakumar, A. R., "Reliability-Based Optimization of Transmission Line Towers," *Computers and Structures*, Vol. 55, No. 3, 1995, pp. 387–403.

[13]Mohareb, M., "Plastic Interaction Relations for Pipe Sections," *Journal of Engineering Mechanics*, Vol. 28, No. 1, 2002 pp. 112–120.

[14]Bushnell, D., "A Strategy for the Solution of Problems Involving Large Deflection, Plasticity and Creep," *International Journal for Numerical Methods in Engineering*, Vol. 11, 1977, pp. 683–708.

[15]Yau, C. Y., Ho, G. W. M., and Chan, S. L., "Elastic-Plastic Large Deflection Analysis of Steel Framed Structures," *Advances in Engineering Plasticity and its Applications*, Elsevier, New York, 1993, pp. 763–770.

[16]Hong, G., "Numerical Analysis of the Large Deflection of an Elastic-Plastic Beam," *Applied Mathematics and Mechanics*, Vol. 21, No. 6, 2000, pp. 699–705.

[17]Yu, T. X., and Hua, Y. L., "Plastic Collapse of Cantilever Beams Under Bending, Shearing and Tension/Compression," *Advances in Engineering Plasticity and Its Applications*, Pergamon, New York, 1996, pp. 845–850.

[18]Al-Bermani, F. G., and Kitipornchai, S. A., "Elasto-Plastic Large Deformation Analysis of Thin-Walled Structures," Dept. of Civil Engineering, Univ. of Queensland, Brisbane, Queensland, Australia, April 1989, pp. 1–33.

[19]Gebbeken, N., "A Refined Numerical Approach for the Ultimate-Load Analysis of 3-D Steel Rod Structures," *Engineering Computations*, Vol. 15, No. 3, 1998, pp. 312–344.

[20]Haldar, A., and Mahadevan, S., "First-Order and Second-Order Reliability Methods," *Probabilistic Structural Mechanics Handbook: Theory and Industrial Applications*, edited by C. R. Sundararajan, Chapman and Hall, New York, 1995, pp. 27–52.

[21]Melchers, R. E., *Structural Reliability Analysis and Prediction*, Melchers/Ellis Horwood, Ltd., New York, 1987, p. 73.

[22]Ayyub, B. M., and Mccuen, R. H., "Simulation-Based Reliability Methods," *Probabilistic Structural Mechanics Handbook: Theory and Industrial Applications*, edited by C. Raj Sundararajan, Chapman and Hall, New York, 1995, pp. 53–69.

[23]Smith, J. O., and Sidebottom, O. M., *Inelastic Behavior of Load-Carrying Members,* Wiley, New York, 1965, pp. 122–129.

[24]Hughes, O. F., *Ship Structural Design,* Wiley, New York, 1983, p. 511.

[25]Megson, T. H. G, *Aircraft Structures for Engineering Students*, Arnold, London, 1999, p. 318.

[26]Nadai, A., *Theory of Flow and Fracture of Solids,* McGraw–Hill, New York, 1950, pp. 490–499.

[27]Drucker, D. C., "Photoelasticity, Plasticity, and Material Behavior," *Applied Mechanics Reviews*, Vol. 54, No. 1, 2001, pp. R1–R10.

[28]Chakrabarty, J., *Theory of Plasticity*, McGraw–Hill, New York, 1987, p. 407.

[29]Yang, T. Y., and Saigal, S., "A Simple Element for Static and Dynamic Response of Beams with Material and Geometric Nonlinearities," *International Journal for Numerical Methods in Engineering*, Vol. 20, 1984, pp. 851–867.

[30]Yang, T. Y., "Matrix Displacement Solution to Elastica Problems of Beams and Frames," *International Journal of Solids and Structures*, Vol. 9, 1973, pp. 829–842.

[31]Vanderplaats, G. N., *Numerical Optimization Techniques for Engineering Design*, Vanderplaats Research and Development, Inc., Colorado Springs, CO, 1999, pp. 229–249.

[32]Ghosh, D. K., Garcelon, J. H., Balabanov, V. O., Venter, G., and Vanderplaats, G., "VisualDoc-a Flexible Design Optimization Software System," AIAA Paper 2000-4931, Sept. 2000.

[33]Ang, A. H-S., and Tang, W. H., *Probability Concepts in Engineering Planning and Design*, Vol. I, Wiley, New York, 1975, pp. 170–218.

[34]Chen, W. F., and Lui, E. M., *Structural Stability: Theory and Implementation,* Prentice–Hall, Upper Saddle River, NJ, 1987, pp. 149–156.

[35]Yang, J. S., Nikolaidis, E., and Haftka, R., "Design of Aircraft Wings Subjected to Gust Loads: a System Reliability Approach," *Computers and Structures*, Vol. 36, No. 6, 1990, pp. 1057–1066.

A. Messac
Associate Editor